Supplementary Figure 1

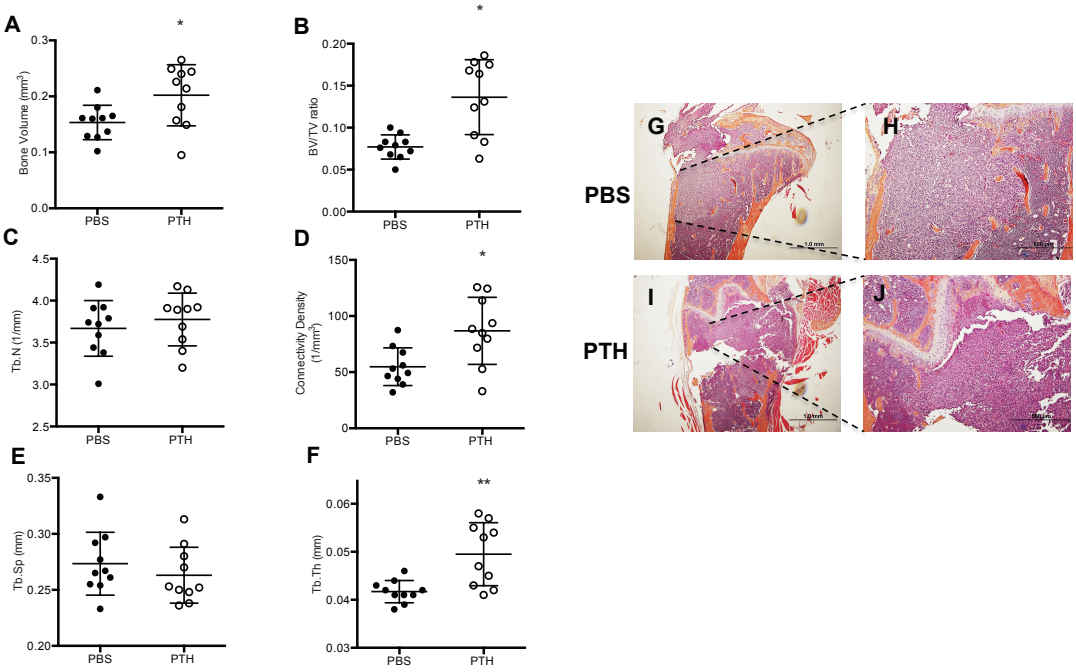

Supplementary Figure 1: PTH treatment increases bone mass in sham-injected hind limbs.

(A) Bone volume, (B) bone volume/tissue volume (BV/TV), (C) trabecular number (Tb.N), (D) connectivity density, (E) trabecular spacing (Tb.Sp), and trabecular thickness (Tb.Th) as measured by μCT in sham-injected proximal tibiae from mice treated with PBS or PTH (intratibial injection model). (G-J) Representative H&E-stained sections of PBS (G and H) and PTH (I and J) treated hind limbs with metastases from the pretreatment model at (G and I) 4x magnification (bar = 1mm) and (H and J) 10X magnification (bar = 500 μM). All values represent mean ± SD of n=10 for each group. *$p < 0.05$, **$p < 0.01$ when compared to PBS group.

Supplementary Figure 2

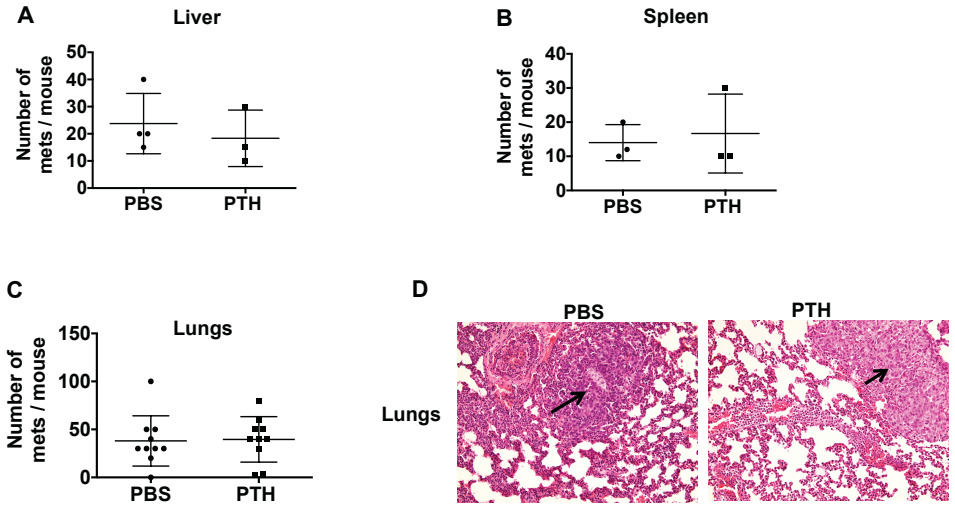

Supplementary Figure 2: Gross and microscopic analyses of metastases to distant organs.

Macroscopic visualization of tumors in (A) liver, (B) spleen, and (C) lungs. (D) Histological analyses of lung at 20X magnification in 4T1 injected mice pre-treated with PBS/PTH (pre-treatment model). All values represent mean ± SD and were not statistically different when compared to the PBS group.

Supplementary Figure 3

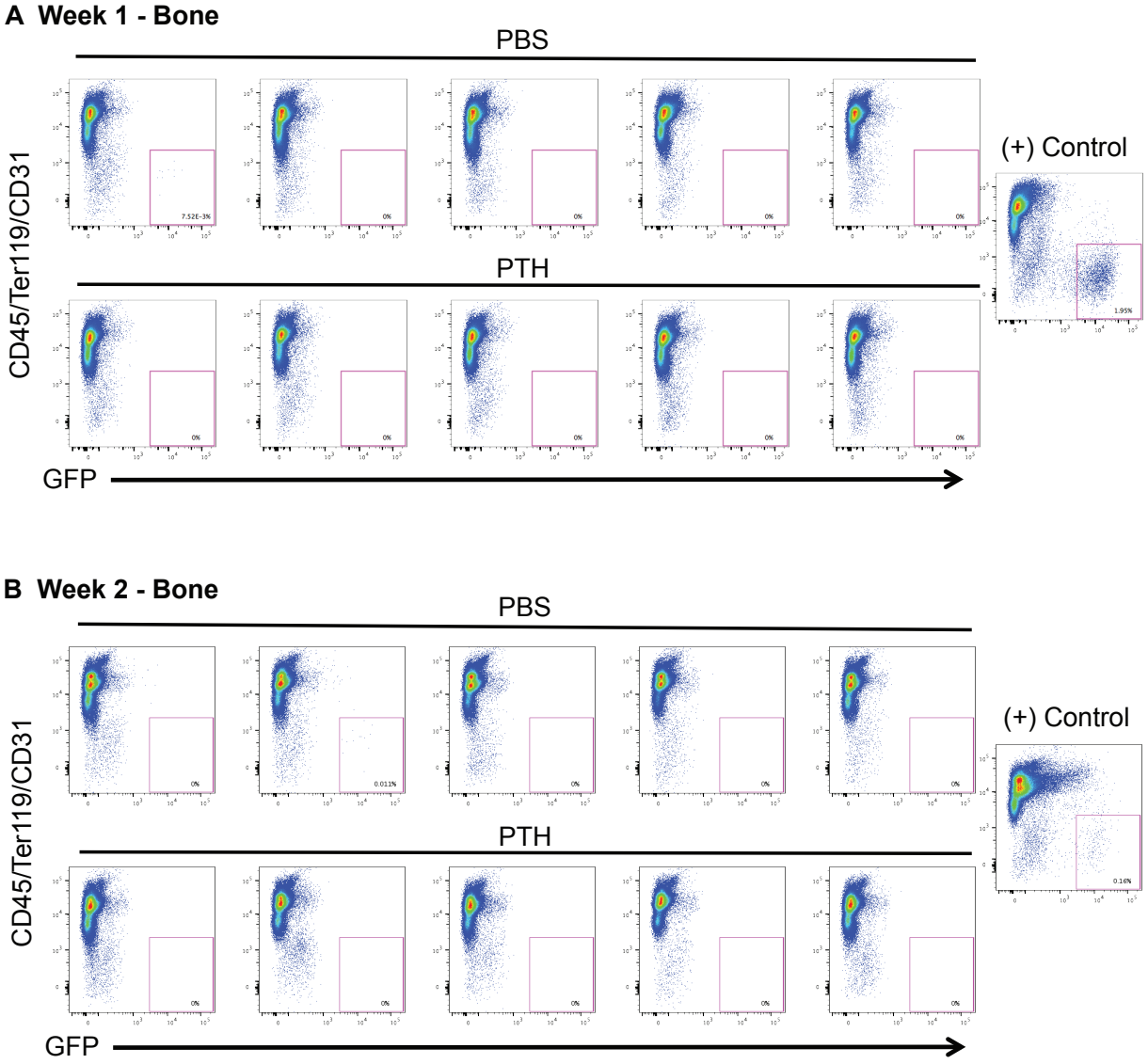

Supplementary Figure 3: Detection of GFP+ 4T1 cells by flow cytometry

Flow cytometry plots for detection of GFP^+ 4T1 cells in PBS and PTH treated mice (n=5) at (A) week 1 and (B) week 2 in hind limb bones. Hind limbs injected intratibially with 4T1 cells were used as positive (+) controls.

Supplementary Figure 4

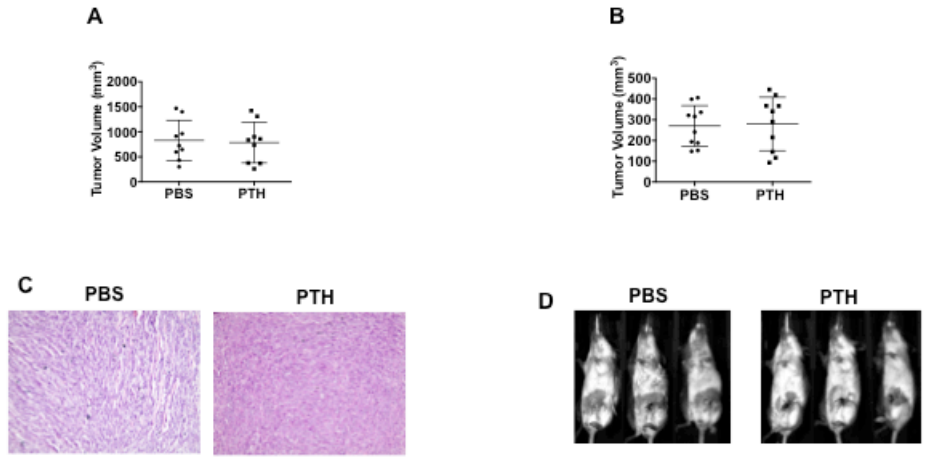

Supplementary Figure 4: Tumor characteristics and wound healing in mice undergoing primary tumor debulking.

Tumor volumes in the experimental groups at time of primary tumor debulking in (A) survival model 1 and (B) survival model 2. (C) Representative H&E staining in primary tumors from survival model 2 and (D) representative mice from survival model 2 showing no BLI signal and equivalent wound healing 5 days post debulking surgery.

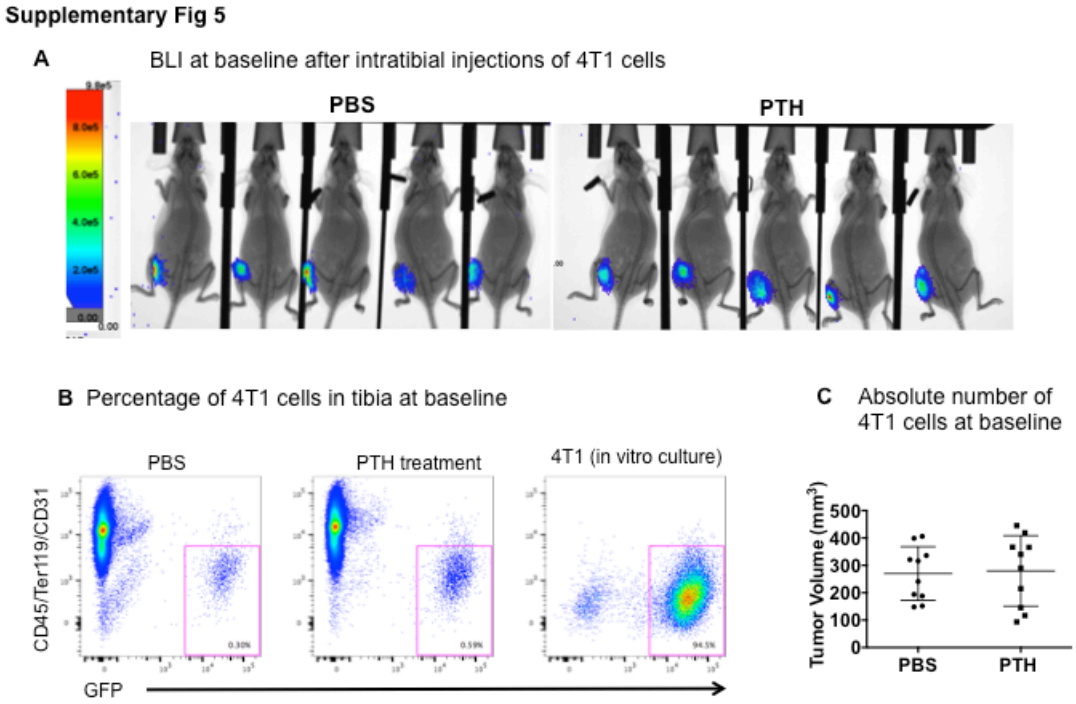

Supplementary Figure 5: Equivalent seeding of 4T1 cells in mice pre-treated with PBS and PTH.

(A) BLI, (B) representative flow cytometry plots for detection of GFP^+ 4T1 cells and (C) absolute numbers of 4T1 cells 6 hours after intratibial injection of 4T1 cells. All values represent means $\pm$ SD (n=10) and were not statistically different when compared to the PBS group.

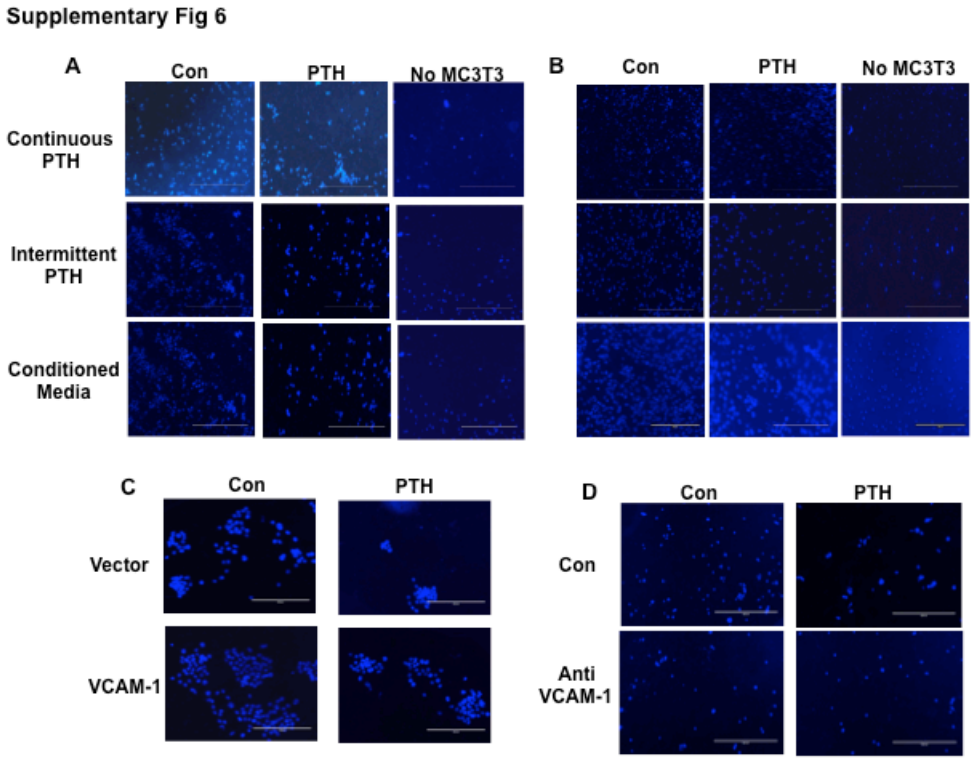

Supplementary Figure 6: Transwell migration of 4T1 and MDA breast cancer cells towards MC3T3-E1 pre-osteoblastic cells.

Representative field views of migration of (A) 4T1 or (B) MDA cells towards MC3T3-E1 pre-osteoblastic cells in transwell assays after 4 hours (10X magnification). Migration of 4T1 cells towards (C) MC3T3-E1 cells overexpressing VCAM-1 or (D) treated with anti VCAM-1 antibody.

Supplementary Table 1: RT2 Profiler Tumor metastasis PCR Array (Qiagen) Gene List , fold change with intermittent PTH treatment and p value

Gene	P Value	Fold Change
Mmp10	0.271840143	-21.39
Cxcl12	0.029376	-20.08
Tgfb1	0.003687	-17.44
Ctsk	0.00394	-17.14
Mmp11	0.006403	-8.6
Mmp13	0.041002	-7.71
Rpsa	0.126100061	-5.98
Hsp90ab1	0.26519838	-5.24
Csf1	0.280424845	-3.16
Pnn	0.07481022	-3.16
Mta1	0.383098278	-3.02
Gusb	0.362983508	-3.01
Plaur	0.281395345	-2.79
Nf2	0.274666102	-2.77
Fxyd5	0.141435844	-2.76
Hras1	0.111552971	-2.63
Nme2	0.190197143	-2.63
Nme1	0.170805477	-2.6
Set	0.176400912	-2.53
Kras	0.129815619	-2.47
Sstr2	0.065136259	-2.44
Pten	0.328477891	-2.28
Ewsr1	0.219884079	-2.24
Nme4	0.37116871	-2.22
Denr	0.173520635	-2.06
Mcam	0.369528925	-2.02
Ctnna1	0.134503132	-1.96
Myc	0.217731616	-1.93
Cd44	0.188176572	-1.86
Mmp2	0.558161428	-1.78
Ephb2	0.129080236	-1.76
Etv4	0.266180423	-1.76
Syk	0.413678296	-1.69
Smad2	0.23153244	-1.63
Fat1	0.567396682	-1.58
Ctsl	0.436173394	-1.53
Src	0.312686413	-1.5
Ctbp1	0.242385565	-1.44
Fn1	0.537621673	-1.38

Cd82	0.39338508	-1.37
Htatip2	0.428254444	-1.36
Mtss1	0.96917124	-1.35
Vegfa	0.344696181	-1.33
Cdh6	0.293320912	-1.32
Cdkn2a	0.293320912	-1.32
Cxcr2	0.293320912	-1.32
Elane	0.293320912	-1.32
Il1b	0.293320912	-1.32
Mdm2	0.328604045	-1.32
Mmp7	0.293320912	-1.32
Smad4	0.175072547	-1.3
Flt4	0.324297945	-1.27
Itgb3	0.575977603	-1.27
Timp2	0.533145589	-1.27
Tcf20	0.370862324	-1.24
Timp3	0.667419355	-1.24
Kiss1	0.502779966	-1.23
Lpar6	0.62902172	-1.22
Itga7	0.64816751	-1.19
Timp4	0.587892009	-1.16
B2m	0.441159501	-1.14
Trp53	0.841732318	-1.12
Il18	0.958963827	-1.1
Mycl	0.814444571	-1.1
Met	0.963430012	-1.07
Chd4	0.756375087	-1.06
Mmp9	0.730711993	-1.06
Igf1	0.922849905	-1.05
Tnfsf10	0.625934376	-1.03
Cdh11	0.964590835	-1.01
Rb1	0.965220876	-1.01
Gpnmb	0.851094951	1.01
Hgf	0.94994707	1.02
Nr4a3	0.730041192	1.02
Actb	0.626693361	1.07
Gapdh	0.775162883	1.07
Col4a2	0.513224433	1.14
Hpse	0.439053484	1.16
Mmp3	0.78464636	1.16
Cdh1	0.541499927	1.17
Ccl7	0.446379193	1.23
Fgfr4	0.593665743	1.25
Cdh8	0.360885438	1.45

Apc	0.348221323	1.47
Rorb	0.344881399	2.24
Cxcr4	0.195724907	2.35
Kiss1r	0.115875471	2.35
Tshr	0.302745445	2.6
Brms1	0.050490311	3.2

Supplementary Table 2: Mouse primer sequences*

Gene	Primer Sequence	Ref
Brms1	Forward 5' - ATTCAGGTGGCAGGGATCTACAAGG 3' Reverse 5' – GCAGCAGCTTCTCACTCTCCA 3'	(1)
βActin	Forward 5' – GATCTGGCACCACACCTTCT 3' Reverse 5' – GGGGTGTTGAAGGTCTCAAA 3'	(2)
COX2	Forward 5' – GGCCTCGTGAGCTTCTTC 3' Reverse 5' – CTTCTGCAGTCCAGGTTCAA 3'	
Ctsk	Forward 5' – ATACGTTACTCCAGTCAAGAACCAG 3' Reverse 5' – TAATTCTCAGTCACACAGTCCACA 3'	(3)
CXCL12	Forward 5' – GAGCCAACGTCAAGCATCTG 3' Reverse 5' – CGGGTCAATGCACACTTGTC 3'	(4)
CXCR4	Forward 5' – TTCTCATCCTGGCCTTCATC 3' Reverse 5' – CTTTTCAGCCAGCAGTTTCC 3'	
CYP19	Forward 5' – CGGAAGAATGCACAGGCTCGAG 3' Reverse 5' – CGATGTACTTCCCAGCACAGC 3'	(5)
IL7	Forward 5' – GGCACACAAACACTGGTGAACT 3' Reverse 5' – TGCATCATTCTTTTTCTGTTCCTT 3'	(6)
IL6	Forward 5' – GAAGATTCCAAAGATGTAGCCG 3' Reverse 5' –TGTTTTCTGCCAGTGCCTC 3'	
KISSr1	Forward 5' – CATGCAGACAGTTACCAA 3' Reverse 5' – CACGCAGCACAGTAGGAAAGT 3'	(7)
MMP10	Forward 5' – CCTGCTTTGTCCTTTGATTCAGT 3' Reverse 5' – CGGGATTCCAATGGGATCT 3'	(8)
MMP11	Forward 5' – CTGTCTCCTCCGCGCGATTT3' Reverse 5' – CAGGAGCCGAGGCCCTTT 3'	(9)
MMP13	Forward 5' – TGATGAAACCTGGACAAGCA 3' Reverse 5' – TCCTCGGAGACTGGTAATGG 3'	(8)
OPG	Forward 5' – GGAACCCCAGAGCGAAACACAGT 3' Reverse 3' – CTTCTTCCCAGGCAGGCTCTCCAT 3'	(10)
p21	Forward 5' – TTGCACTCTGGTGTCTGAGC 3' Reverse 5' – GGGCACTTCAGGGTTTTCTC 3'	
PTHrP	Forward 5' – TTCAGCAGTGGAGTGTCCTG 3' Reverse 5' – GATGGACTTGCCCTTGTCAT 3'	
RANKL	Forward 5' – GCTTCACTGCCCAGTCTCATCGTT 3' Reverse 5' – GGGCCGGTCCGTGTACTCATCCT 3'	(10)
TGFβ	Forward 5' – ATACTAAAGAGGTCACCCGC 3' Reverse 5' – TGCTTCCCGAATGTCTGACG 3'	
TNFα	Forward 5' – AGGCGGTGCTTGTTCCTCAG 3' Reverse 5' – TACAGGCTTGTCACTCGGGG 3'	
VCAM1	Forward 5' – TGACAAGTCCCCATCGTTGA 3' Reverse 5' – ACCTCGCGACGGCATAATT 3'	(11)
VEGFR1	Forward 5' – GTCTCCATCAGTGGCTCTACG 3' Reverse 5' – CCCGGTTCTTGTTGTATTTTG 3'	

* All primers were designed using MacVector Version12.6 software unless indicated otherwise.

REFERENCES

1. Ma H, and Gollahon LS. ERalpha Mediates Estrogen-Induced Expression of the Breast Cancer Metastasis Suppressor Gene BRMS1. Int J Mol Sci. 2016;17(2).
2. Bastepe M, Weinstein LS, Ogata N, Kawaguchi H, Juppner H, Kronenberg HM, and Chung UI. Stimulatory G protein directly regulates hypertrophic differentiation of growth plate cartilage in vivo. Proceedings of the National Academy of Sciences of the United States of America. 2004;101(41):14794-9.
3. Hao L, Chen W, McConnell M, Zhu Z, Li S, Reddy M, Eleazer PD, Wang M, and Li YP. A small molecule, odanacatib, inhibits inflammation and bone loss caused by endodontic disease. Infect Immun. 2015;83(4):1235-45.
4. Semerad CL, Christopher MJ, Liu F, Short B, Simmons PJ, Winkler I, Levesque JP, Chappel J, Ross FP, and Link DC. G-CSF potently inhibits osteoblast activity and CXCL12 mRNA expression in the bone marrow. Blood. 2005;106(9):3020-7.
5. Zhao H, Innes J, Brooks DC, Reierstad S, Yilmaz MB, Lin Z, and Bulun SE. A novel promoter controls Cyp19a1 gene expression in mouse adipose tissue. Reprod Biol Endocrinol. 2009;7(37.
6. Blin-Wakkach C, Wakkach A, Quincey D, and Carle GF. Interleukin-7 partially rescues B-lymphopoiesis in osteopetrotic oc/oc mice through the engagement of B220+ CD11b+ progenitors. Experimental hematology. 2006;34(7):851-9.
7. Merhi Z, Thornton K, Bonney E, Cipolla MJ, Charron MJ, and Buyuk E. Ovarian kisspeptin expression is related to age and to monocyte chemoattractant protein-1. J Assist Reprod Genet. 2016;33(4):535-43.
8. Ai F, Zhang X, Li X, Qin Z, Ye Q, Tian L, Tang A, Li N, Li G, Ma J, et al. Up-regulation of matrix metalloproteinases in a mouse model of chemically induced colitis-associated cancer: the role of microRNAs. Oncotarget. 2015;6(7):5412-25.
9. Lafleur MA, Drew AF, de Sousa EL, Blick T, Bills M, Walker EC, Williams ED, Waltham M, and Thompson EW. Upregulation of matrix metalloproteinases (MMPs) in breast cancer xenografts: a major induction of stromal MMP-13. International journal of cancer. 2005;114(4):544-54.
10. Kenner L, Hoebertz A, Beil FT, Keon N, Karreth F, Eferl R, Scheuch H, Szremska A, Amling M, Schorpp-Kistner M, et al. Mice lacking JunB are osteopenic due to cell-autonomous osteoblast and osteoclast defects. The Journal of cell biology. 2004;164(4):613-23.
11. Hosking BM, Wang SC, Downes M, Koopman P, and Muscat GE. The VCAM-1 gene that encodes the vascular cell adhesion molecule is a target of the Sry-related high mobility group box gene, Sox18. The Journal of biological chemistry. 2004;279(7):5314-22.